Provisional Assessment of Candidate High-Temperature Thermal Conductivity Reference Materials in the EMRP "Thermo" Project

J. Wu, jiyu.wu@npl.co.uk, R. Morrell, roger.morrell@npl.co.uk, T. Fry, tony.fry@npl.co.uk, S. Gnaniah, sam.gnaniah@npl.co.uk, D. Gohil, dipak.gohil@npl.co.uk, and A. Dawson, angela.dawson@npl.co.uk
National Physical Laboratory (NPL), United Kingdom
J. Hameury, jacques.hameury@lne.fr, and A. Koenen, alain.koenen@lne.fr
Laboratoire National de Métrologie et d'Essais (LNE), France
U. Hammerschmidt, ulf.hammerschmidt@ptb.de
Physikalisch-Technische Bundesanstalt (PTB), Germany
E. Turzó-András, thurzo-a@mkeh.hu
Magyar Kereskedelmi Engedélyezési Hivatal (MKEH), Hungary
R. Strnad, rstrnad@cmi.cz, and A. Blahut, ablahut@cmi.cz
Český Metrologický Institut (CMI), Czech Republic

ABSTRACT

This article describes the provisional assessment of a short list of four candidate high-temperature thermal conductivity reference materials in a European research project, "Thermo." These four candidate materials are low-density calcium silicate, amorphous silica, high-density calcium silicate, and exfoliated vermiculite. Based on initial tests on material composition and microstructure changes, dimensional stability, mechanical stability, chemical stability and uniformity, the best two candidate materials that would be considered for further detailed characterization in the next stage are low-density calcium silicate and high-density calcium silicate. These two materials are dimensionally, mechanically, and chemically stable, which are more robust and easier to handle than others. However, the specimens need to be selected to meet the requirement for material uniformity in terms of density, i.e., density variation within 2%.

Keywords: thermal conductivity, reference material, provisional assessment, high temperature, dimensional stability, mechanical stability, chemical stability, uniformity.

1. INTRODUCTION

Within the European Union (EU), regulations (EU NO. 305/2011) and harmonized EN product standards (EN 14303 to EN 14309, EN 14313, and EN 14314) have recently been issued by the European Committee for Standardization (CEN). It became mandatory in August 2012 that manufacturers must declare the performance values defined in these regulations before they can market their thermal insulation products within Europe. Thermal conductivity is the key performance value that must be declared. However, currently, it is impossible for the manufacturers to declare the thermal conductivity values with a required resolution that is three times better than the current level of agreement between national reference laboratories (Salmon, Tye, & Lockmuller, 2009; Tye & Salmon, 2002; Wu & Morrell, 2012; Wu, Salmon, Lockmuller, Stacey, & Gaal, 2010). Measurement of thermal conductivity using different techniques can often produce scatter of over 100% (Ebert & Hemberger, 2011), which means advanced manufacturing industries cannot reliably

select or develop thermal protection materials for their engineering applications. However, there is no high-temperature reference material available with an appropriate level of thermal conductivity (0.02 W m^{-1} K^{-1} to 1 W m^{-1} K^{-1}) that could be used to aid in the investigation of disagreements between laboratories, and to achieve an European equivalency that is three times better than the current state-of-the-art.

To support the implementation of the new European regulations and to resolve the discrepancies, five European National Measurement Institutes (NPL, LNE, PTB, MKEH, and CMI) have started a Joint Research Project, "Thermo" that is funded by the European Metrology Research Program (EMRP). One of the aims of this project is to develop reference materials with thermal conductivity in the range 0.02 W m^{-1} K^{-1} to 1 W m^{-1} K^{-1} and with a target maximum temperature of $800°C$. The required reference materials should satisfy the requirements of the ISO Guide 34 (ISO, 2009) guidelines for long-term property stability/uniformity/reproducibility, should be

robust, and enable the comparison of different types of apparatus. The development of the reference materials consists of three stages: provisional assessment of candidate reference materials; detailed assessment of candidate reference material(s); and inter-laboratory comparisons and data analysis for material certification.

This article describes the provisional assessment of a short list of four candidate high-temperature thermal conductivity reference materials. They are selected based on results of literature reviews (Tye & Salmon, 2002; Ebert & Hemberger, 2011; Salmon, 2001) and surveys that were sent to reference laboratories and to international insulation and refractory manufacturers at the start of the "Thermo" project. These four candidate materials are low-density calcium silicate (LDCaSi), amorphous silica (AmSi), high-density calcium silicate (HDCaSi-N), and exfoliated vermiculite (EV). The aim of the provisional tests is to select one or two best candidate reference materials for further detailed assessment within the next stage. The selection is based on a test matrix including material dimensional stability, mechanical stability, chemical stability, uniformity, and isotropic aspects of each material.

2.   PROVISIONAL ASSESSMENT

2.1 Material composition and microstructure

To understand the behavior of each material, it is essential to know its chemical composition and microstructure, in particular its stability under thermal cycling. In this article, the results of X-ray fluorescence spectrometry (XRF), and X-ray diffraction (XRD) reveal the composition of each material. The microstructure of each material, before and after heat treatment, is illustrated in the micrographs obtained using a scanning electron microscope (SEM).

2.1.1 Elementary composition – XRF results

To reveal the elementary composition, chemical analysis using XRF has been carried out on all four refractory type candidate materials and two additional types of high-density calcium silicate, HDCaSi-B and HDCaSi-HT3B. This last material is from the same batch as the internal audit specimens that the National Physical Laboratory has used for more than a decade (Salmon, 1996).

The XRF elements analysis (Table 1) includes SiO_2, TiO_2, Al_2O_3, Fe_2O_3, CaO, MgO, K_2O, Na_2O, P_2O_5, Cr_2O_3, Mn_3O_4, ZrO_2, HfO_2, PbO, ZnO, BaO, SrO, SnO_2, and CuO. Please note that SO_3 remaining in the bead after loss and fusion is also reported, but this is not a total SO_3 figure. A result for loss on ignition is also reported.

2.1.2 Main components – XRD results

To analyze the main components of each candidate material, XRD measurements were performed on samples before and after being held 24 hours in a thermogravimetric analysis apparatus (TGA-Cahn TG-171) at 850°C for three cycles. The measurements were performed using a Siemens D5000 diffractometer using Cu-Kα radiation. Table 2 summarizes the XRD data with the major phases identified in the X-ray diffraction before and after the heat treatment conducted in the TGA. In all cases, the XRD data showed that after heat treatment, the diffraction peaks are better resolved and "sharper," indicating that amorphous phases have been removed and the diffracting crystallites refined. A typical example of the diffraction data is presented in Figure 1; the major phases identified and listed in Table 2 are also shown in this figure.

2.1.3 Microstructure – SEM micrographs

All four candidate materials were examined using SEM to assess if there had been any significant changes to their microstructures as a result of heat treatment and thermal cycling, which could affect thermal properties. The first heat treatment of each sample was carried out up to 850°C in an air environment for 24 hours. The thermal cycling was carried out as three runs up to 850°C in air and held for 24 hours in the TGA. A Camscan MX2500 SEM fitted with a backscattered electron detector was used for microstructural characterization work.

To examine the internal microstructures, all the samples were fractured in two orthogonal directions. Through-thickness and in-plane fractures of the as received, after first heat treatment, and post-TGA characterized samples (after three runs in the TGA) were prepared and then gold coated to reduce "charging" effects in the SEM.

Backscattered electron images of all samples were acquired at a nominal magnification of 100×. The images for LDCaSi and HDCaSi-N samples only are shown in Figures 2 and 3. The images labeled as (a) and (b) show the as received in-plane and the through-thickness fracture surfaces, respectively. The images labeled as (c) and (d) show the samples after the first heat treatment as in-plane and through-thickness fracture surfaces, respectively. The images labeled as (e) and (f) show the samples after three runs in the TGA as in-plane and through-thickness fracture surfaces, respectively. In Figure 2, organic fibers have been burnt out after the first heat treatment (see Figure 2c and 2d), and the microstructure remains stable after three runs in the TGA (see Figure 2c–2f). Figure 3c–3f shows some circular black features, which have been identified as the holes formed by melting of the glass fibers seen in Figure 3b. Again the microstructure of

Table 1. The oxide composition of each material.

Result(s)		LDCaSi	AmSi	EV	HDCaSi-N	HDCaSi-B	HDCaSi-HT3B*
Sample basis		Dried 110°C	Dried 110°C	Dried 110°C	Dried 110°C	Dried 110°C	Dried 110°C
Silicon dioxide	SiO_2	45.72%	65.86%	46.98%	48.53%	54.05%	51.85%
Titanium dioxide	TiO_2	0.01%	31.25%	0.36%	0.18%	0.06%	0.03%
Aluminum oxide	Al_2O_3	0.15%	1.01%	10.20%	0.62%	0.59%	0.49%
Iron (III) oxide	Fe_2O_3	0.10%	0.28%	5.13%	0.22%	0.45%	0.33%
Calcium oxide	CaO	43.99%	0.01%	2.01%	44.12%	42.54%	45.62%
Magnesium oxide	MgO	0.58%	<0.02%	20.47%	0.33%	0.17%	0.35%
Potassium oxide	K_2O	0.12%	<0.01%	2.89%	0.28%	0.03%	0.15%
Sodium oxide	Na_2O	<0.03%	<0.03%	2.73%	0.34%	0.04%	0.40%
Phosphorus pentoxide	P_2O_5	0.05%	<0.02%	0.31%	0.03%	0.03%	0.04%
Chromium (III) oxide	Cr_2O_3	<0.01%	0.09%	<0.01%	<0.01%	<0.01%	<0.01%
Manganese (II,III) oxide	Mn_3O_4	0.03%	<0.01%	0.09%	0.04%	0.09%	0.08%
Zirconium oxide	ZrO_2	0.68%	0.30%	<0.02%	0.59%	<0.02%	0.59%
Hafnium (IV) oxide	HfO_2	0.01%	<0.01%	<0.01%	0.01%	<0.01%	0.01%
Lead oxide	PbO	<0.02%	<0.02%	<0.02%	<0.02%	<0.02%	<0.02%
Zinc oxide	ZnO	<0.01%	<0.01%	0.01%	0.01%	<0.01%	<0.01%
Barium oxide	BaO	<0.01%	<0.01%	0.04%	<0.01%	<0.01%	0.01%
Strontium (II) oxide	SrO	0.01%	<0.01%	0.01%	<0.01%	0.01%	<0.01%
Tin (IV) oxide	SnO_2	<0.01%	<0.01%	<0.01%	<0.01%	<0.01%	<0.01%
Copper oxide	CuO	<0.01%	<0.01%	<0.01%	<0.01%	<0.01%	0.02%
Loss on ignition		8.16%	1.10%	8.53%	4.38%	2.02%	0.11%
Loss on ignition temperature °C		1025	1025	1025	1025	1025	1025
Total		99.61%	99.90%	99.76%	99.68%	100.08%	100.08%
Sulfur trioxide	SO_3	0.13%	<0.05%	<0.05%	0.10%	<0.05%	<0.05%
SiO_2/CaO ratio		**1.04**			**1.10**	**1.27**	**1.14**

*The HDCaSi-HT3B sample had been heated to 1100°C before sending for XRF analysis.

Table 2. Major phases identified using x-ray diffraction on the as-received and heat treated refractory samples.

Material ID	Major phases identified	
	As-received	**After heat treatment**
LDCaSi	Xonotlite ($Ca_6Si_6O_{17}(OH)_2$)	Wollastonite
AmSi	Rutile (TiO_2)	Rutile
EV	Vermiculite $(Mgx(Mg,Fe)_3 (Si,Al)_4O_{16}(OH)_2 \cdot 4H_2O)$	Vermiculite
HDCaSi-N	Hydrated calcium silicate ($Ca_2SiO_4 \cdot H_2O$) Quartz	Calcium silicate Quartz
HDCaSi-B	Wollastonite ($CaSiO_3$) Quartz (SiO_2)	Wollastonite Quartz

Figure 1. X-ray diffraction trace for LDCaSi showing the diffraction data before and after the heat treatment.

HDCaSi-N remains stable after three runs in the TGA. Comparing Figures 2 and 3, the HDCaSi-N shows a more anisotropic structure than LDCaSi.

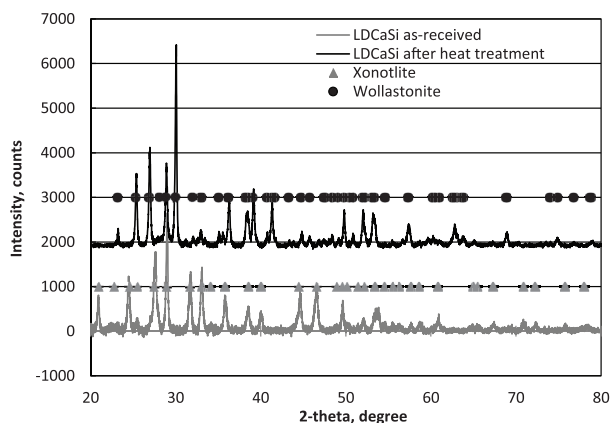In both of these materials, the fine-scale nature of the microstructures, in particular of the $CaSiO_3$ phase, remains after the heat treatment and three thermal
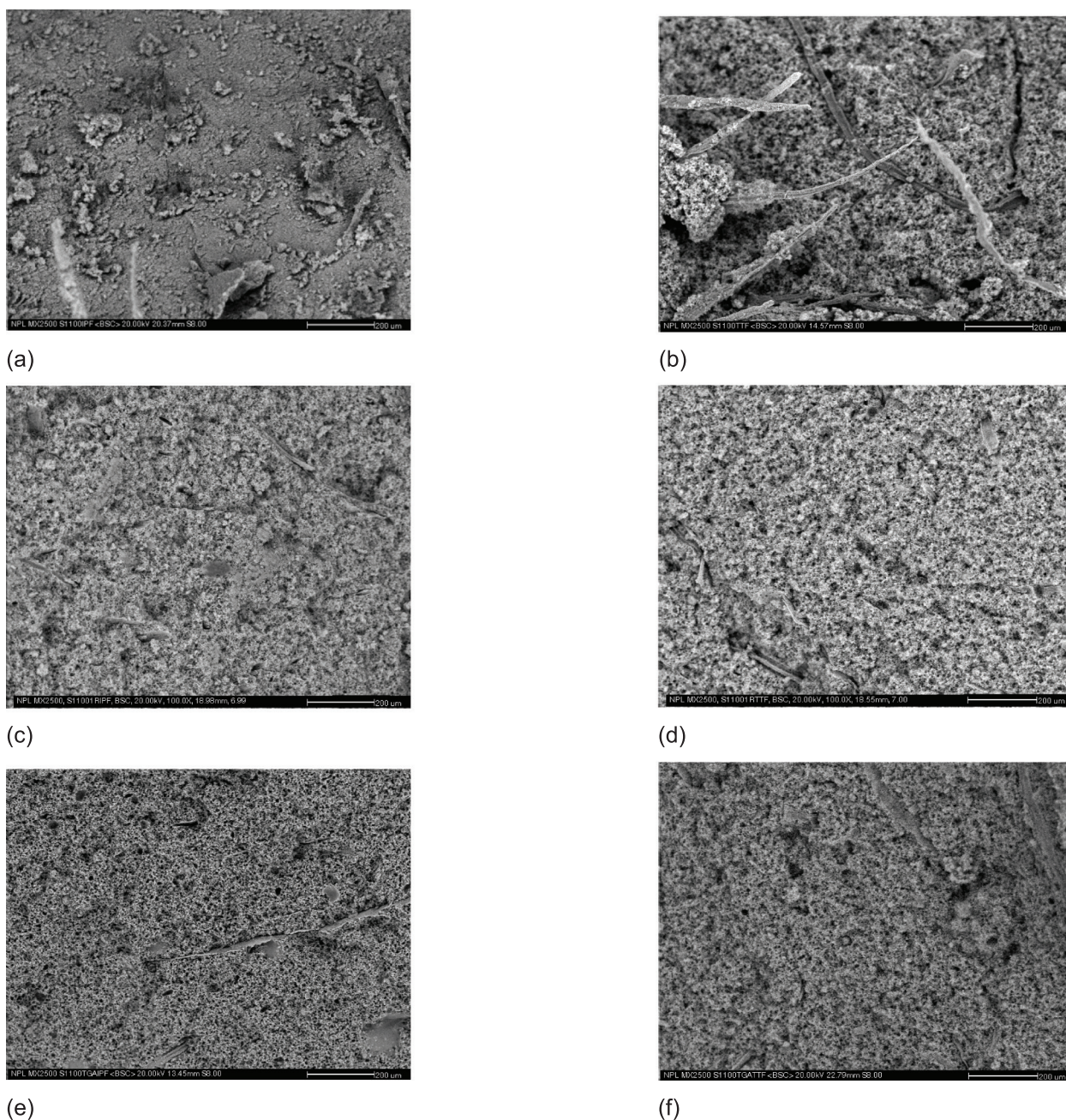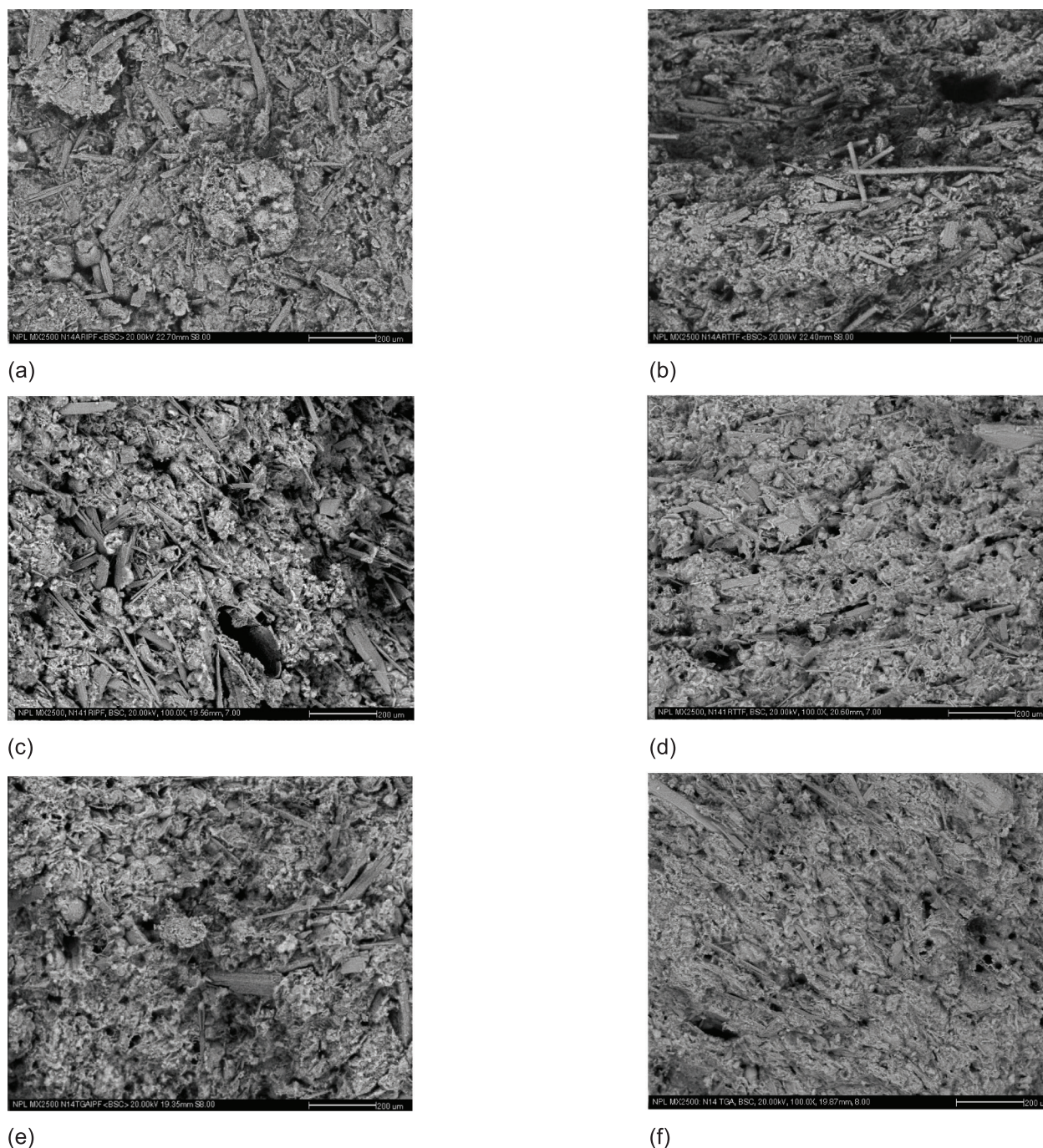
(a)

(b)

(c)

(d)

(e)

(f)

Figure 2. Backscattered electron images of fractured surfaces of LDCaSi: (a) as received, in-plane; (b) as received, through thickness; (c) after first heat treatment at 850°C for 24 hours, in-plane; (d) after first heat treatment at 850°C for 24 hours, through thickness; (e) post TGA, in-plane; and (f) post TGA, through thickness.

cycling, indicating that there are good prospects for the long-term stability of properties.

2.2 Mechanical stability under thermal cycling and isotropy aspects

The investigation of material mechanical stability under thermal cycling and isotropy aspects of each material is through thermal expansion tests. Results of three repeated thermal expansion tests along the in-plane and through-thickness directions are presented in the article. For each candidate material, the measured thermal expansion data are then compared with the measured shrinkage of a larger size specimen after heat treatment in air up to 850°C (or 750°C for EV) for 24 hours.

2.2.1 Thermal expansion
Thermal expansion measurements were made using a Linseis twin push-rod alumina dilatometer calibrated using platinum and alumina reference materials. Test pieces ~30 mm in length and 5–6 mm^2 were carefully cut using a small saw or a knife (for AmSi). In the test apparatus, a small axial force of 50 mN (for AmSi) or

(a)

(b)

(c)

(d)

(e)

(f)

Figure 3. Backscattered electron images of fractured surfaces of HDCaSi-N: (a) as received, in-plane; (b) as received, through thickness; (c) after first heat treatment at 850°C for 24 hours, in-plane; (d) after first heat treatment at 850°C for 24 hours, through thickness; (e) post TGA, in-plane; and (f) post TGA, through thickness.

150 mN was applied. They were then subjected to three thermal cycles to 850°C at a heating and cooling rate of 2°C min^{-1} with a 1-hour hold at peak temperature. The results are shown in Figure 4. All materials underwent significant shrinkages both in-plane and through-thickness in the first thermal cycle, the latter direction usually showing greater changes. Materials LDCaSi and HDCaSi-N showed the least changes after the first thermal cycle. Material AmSi proved to

be very difficult to handle and was extremely fragile with large apparent in-plane shrinkage. Materials EV and HDCaSi-B showed the development of cristobalite after the first thermal cycle, identified from the kink in the traces at about 200°C.

2.2.2 Thermal shrinkage of large specimens
The thermal shrinkage of each candidate material was measured on a large size specimen with nominal
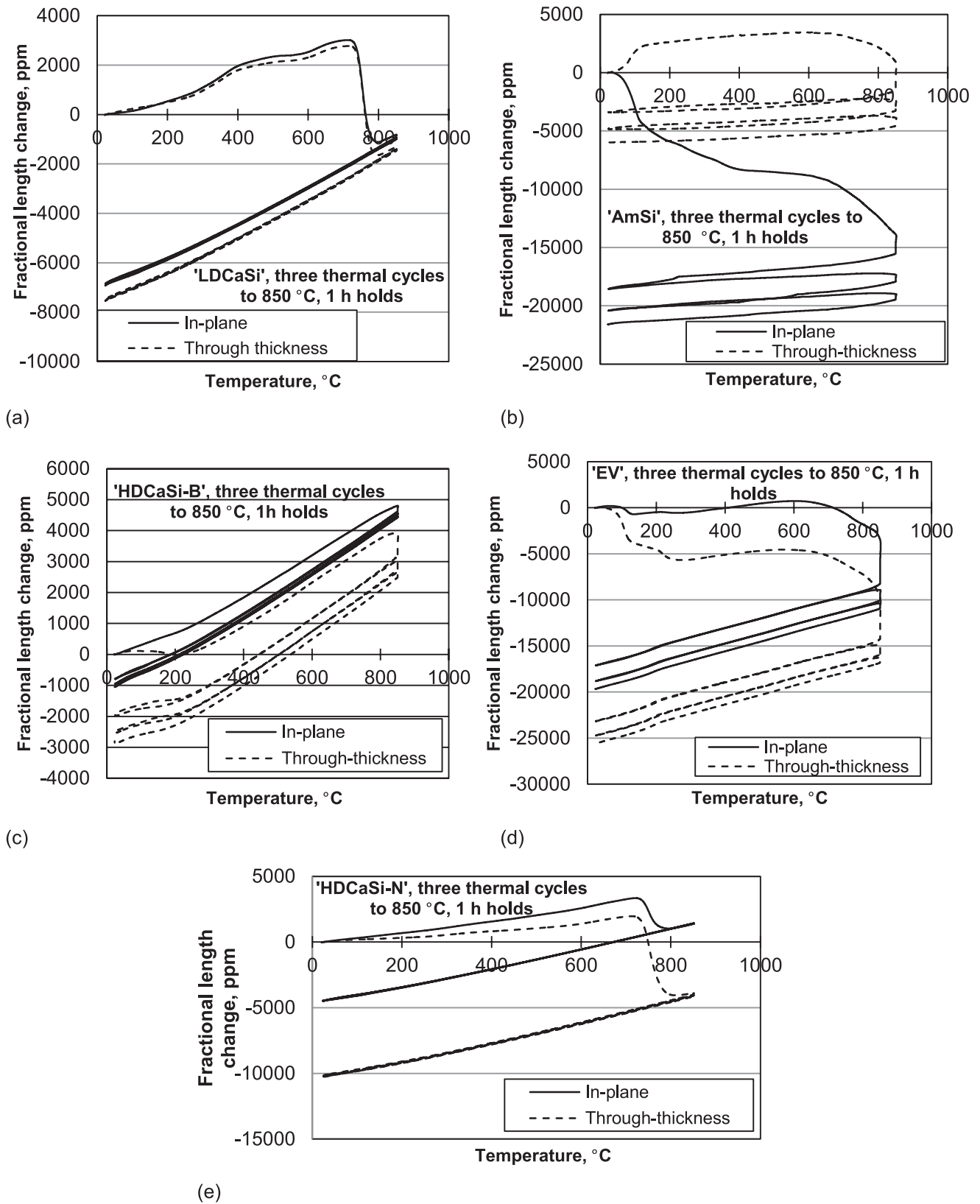
(a)

(b)

(c)

(d)

(e)

Figure 4. Thermal expansion of (a) LDCaSi; (b) AmSi; (c) HDCaSi-B; (d) EV; and (e) HDCaSi-N.

dimensions of 300 mm × 300 mm × 50 mm. The top and bottom surfaces of each specimen were ground flat and parallel within 0.03 mm. Each specimen was then heat treated at 850°C (or 750°C for EV) for 24 hours, free of compressive load. The thermal shrinkage rate is obtained by comparing the lateral and thickness dimensions of each specimen before and after the heat treatment.
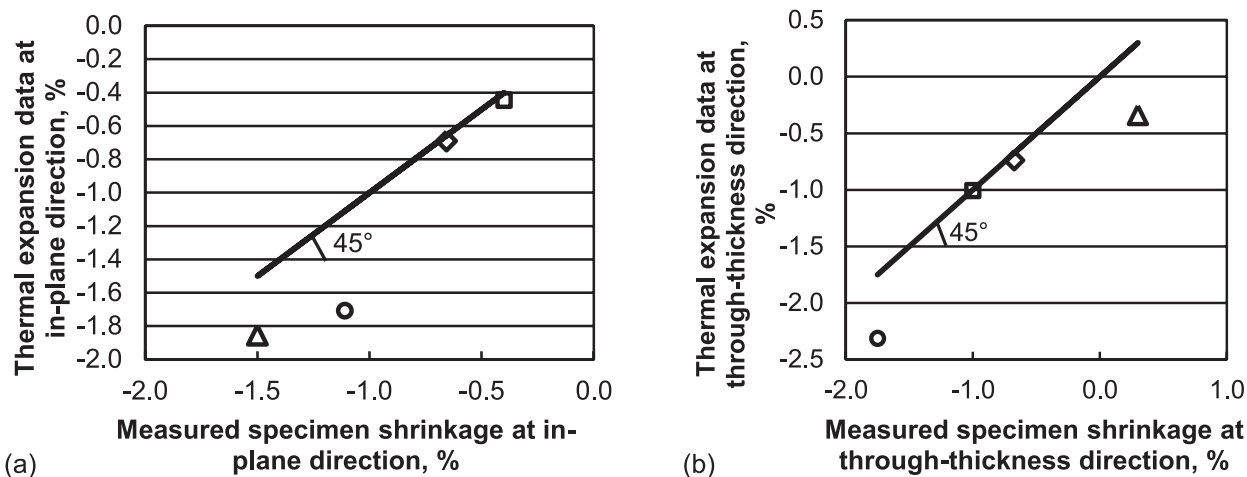
Figure 5. Comparison between the measured specimen shrinkage and the thermal expansion data: (a) at in-plane direction; (b) at through-thickness direction.

For each candidate material, the thermal shrinkage was compared with the thermal expansion data, and the results are shown in Figure 5, with (a) for in-plane direction and (b) for through-thickness direction. The square symbol represents HDCaSi-N; the diamond symbol represents LDCaSi; the circle symbol represents EV; and the triangle symbol represents AmSi. The solid line is plot at 45° angle where the values from thermal expansion data equal the values of measured shrinkage. The samples in thermal expansion tests appear to shrink more than those in thermal shrinkage tests, particularly for AmSi and EV materials. This is because in the thermal expansion tests, the samples were under some compressive load (a few kPa), and the fragile nature of AmSi and EV made them more sensitive to load.

It is worth mentioning that after the first heat treatment, only the surfaces of the LDCaSi specimen remain flat and parallel within 0.03 mm, all other specimens were found slightly warped. However, after grinding the surfaces of the heat treated AmSi, HDCaSi-N, and EV specimens flat and parallel within 0.03 mm, they stay flat after being through two repeated thermal cycling up to 850°C (or 750°C for EV) at 1°C·min^{-1} rate.

2.3 Chemical stability under thermal cycling

The chemical stability under thermal cycling is evaluated through the mass changes measured in a TGA and through heat changes measured in a differential scanning calorimeter (DSC).

2.3.1 TGA results
Two different TGA apparatus, TA Instruments Q5000 IR and Cahn TG-171, were used to assess the chemical stability of each material under thermal cycling. The TA Instruments Q5000 IR with balance sensitivity better than 0.1 μg was used to determine the weight changes in a material as a function of temperature in a flowing air (flow rate 25 ml min^{-1}) environment.

Each sample was placed in an alumina crucible and kept in equilibrium with the test environment at 35°C, and thereafter heated in an air environment at a rate of 3°C·min^{-1} up to 850°C. However, this apparatus is not able to hold the sample at 850°C for long periods and thus might lead to incomplete chemical reactions, as shown in Figure 6a for LDCaSi. Figure 6 shows three repeated TGA tests in a TA Instruments Q5000 IR for the same samples of LDCaSi (Figure 6a) and HDCaSi-N (Figure 6b) – the mass of a sample reduces when temperature increases. This is likely caused by the loss of water and organic binder at lower temperatures and the burning off of organic binder and fiber and material changes at higher temperatures.

The TGA, Cahn TG-171, with 100 g capacity and 20 μg balance resolution was used to check if the initial thermal treatment had been successful at removing the binder or other reactive phases present. Unlike the TA Instruments Q5000 IR, the Cahn TG-171 can hold the specimen at 850°C for long periods. During the tests, a large rectangular block of each material with dimensions of 50 mm × 20 mm × 10 mm was suspended in the measurement zone. It was then heated in a flowing air environment (flow rate 60 ml·min^{-1}) up to 850°C at a 1°C·min^{-1} rate and was held at this temperature for 24 hours prior to cooling. Two additional repeat TGA runs were then performed on the same sample. Figure 7 shows the mass loss of each sample of the candidate materials at the end of 24 hours holding at 850°C in each run. For each material, the mass change finishes after the first TGA run and the results of the second and third run show that the mass of each sample is stable.

2.3.2 DSC results
In order to assess the chemical stability of the candidate materials, in particular the stability after the first heat treatment, thermal analysis was performed using a Netzsch 404 F1 DSC. It measures the heat absorbed
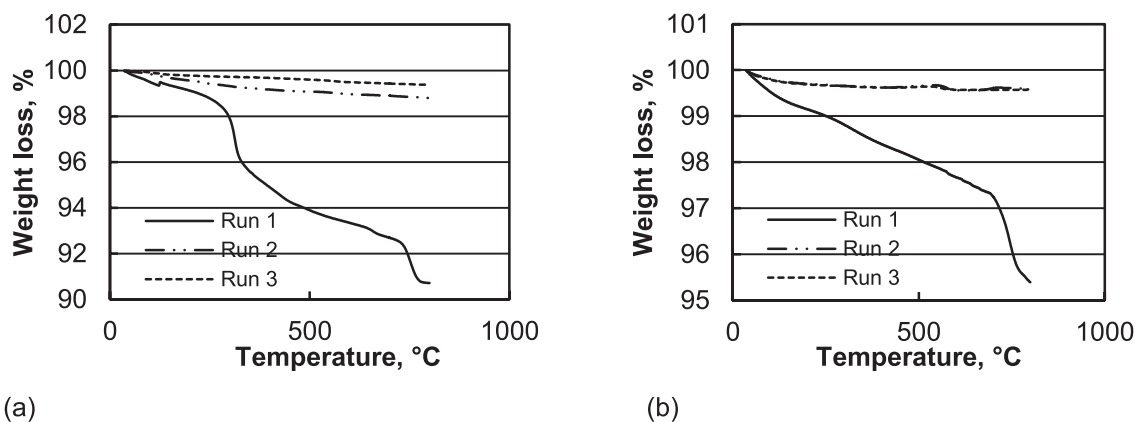
Figure 6. Three repeated TGA tests for the same samples of (a) LDCaSi and (b) HDCaSi-N.
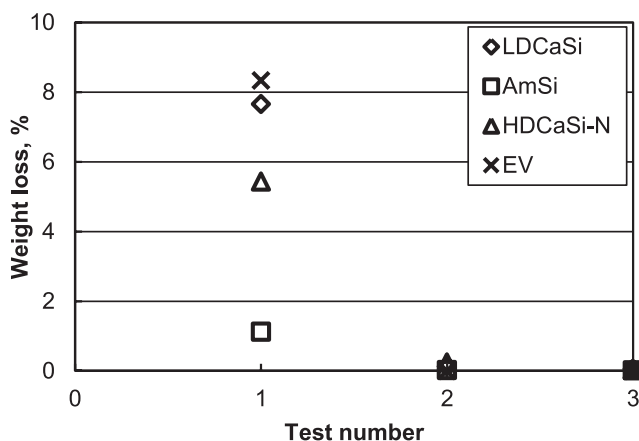

Figure 7. Weight loss after each run in the TGA (Cahn TG-171), where samples were held at 850°C for 24 hours.

(endothermic process) or given off (exothermal effect) by a sample, as it is heated or cooled in a static air environment.

Each material was tested over three heating and cooling cycles from 40°C to 875°C at 5°C min^{-1} heating and cooling rates. The heat flow signal was logged as a function of temperature and recorded as normalized heat flow signal with respect to sample mass. The results in Figure 8 show significant features on first heating of the samples, but thereafter the behavior is stable. The features in the first heating are complex and are likely to be due to a combination of processes including loss of water of hydration, burn out of organics and phase changes.

2.4 Material uniformity

The assessment of material uniformity is based on the density distribution measured before heat treatment. For each material, the measured data are reported in Figure 9 on the density variation within one board; between at least two boards from the same production batch; and between two batches for AmSi and LDCaSi.

The density of each specimen is compared with the specimen that has the minimum density within all the specimens of that material. The nominal dimensions of each specimen used in the uniformity assessment are shown in Table A.1 in the Appendix. The criteria for assessing material uniformity are set according to the new European technical specification for determination of thermal resistance by means of guarded hot plate method, CEN/TS 15548-1:2014 (CEN, 2014). For same size specimens if their thickness and mass differ by less than 2%, then the specimens could be considered as identical. The thickness requirement can be met by machining the specimens. However, the specimens need to be selected to meet the requirement for material uniformity in terms of density, i.e., the measured density variation is within 2%.
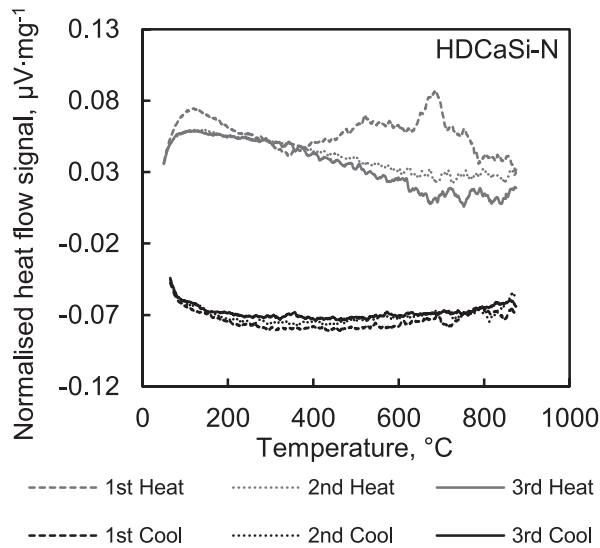
For the candidate material LDCaSi, 15 specimens were machined from two batches of boards. There are 11 specimens that were machined from three boards (board No. "a" to "c") produced in one batch and four specimens that were machined from three boards (board No. "d," "e," and "f") produced in another batch. Each board has nominal dimensions of 1250 mm × 500 mm × 50 mm. As shown in Figure 9(a), maximum 9 out of 15 specimens would meet the criteria of density variation within 2% (see the 4%–6% band).

For the candidate material AmSi, 11 specimens were machined from two batches of boards. Except the specimen No. h-1, the remaining 10 specimens were machined from the six boards (No. "a" to "f") produced in the same batch. Each board has nominal dimensions of 500 mm × 500 mm × 50 mm. As shown in Figure 9(b), maximum 7 out of 11 specimens would meet the criteria of density variation within 2% (see the 0%–2% band).
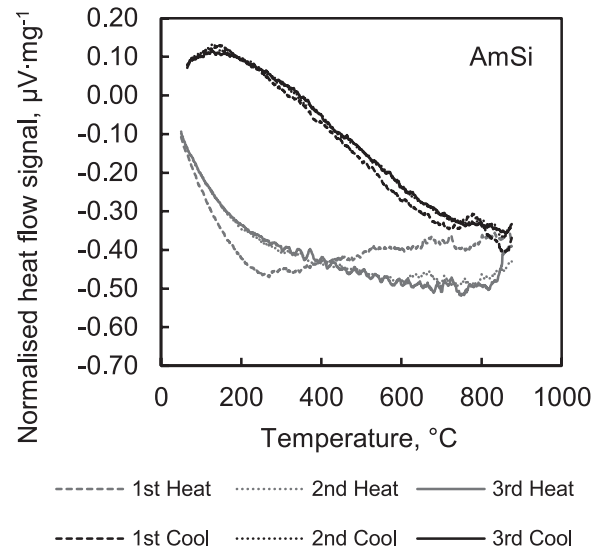
For the candidate material HDCaSi-N, 24 specimens were machined from two boards ("a" and "b") produced in same batch. The board "a" has nominal dimensions of 2570 mm × 1270 mm × 50 mm, and the board "b"
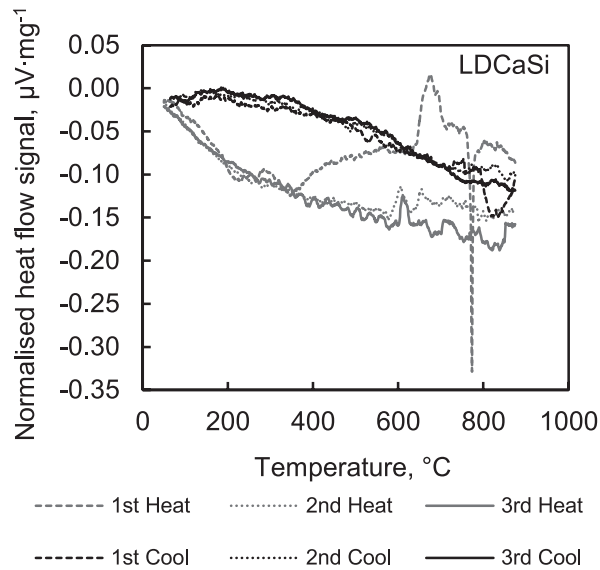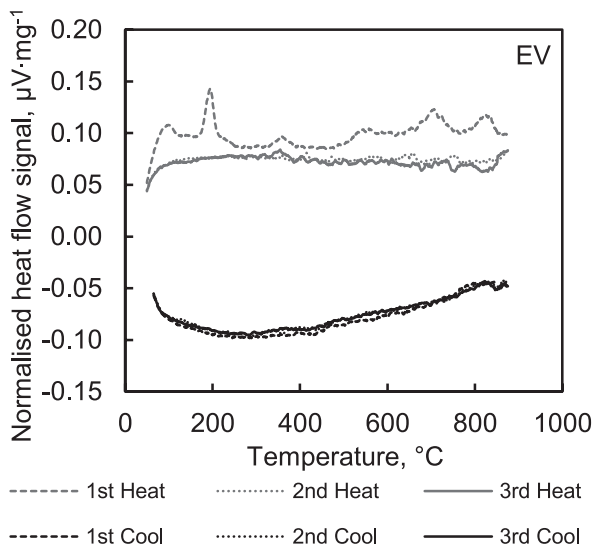
Figure 8. The DSC test results for each candidate material.

has nominal dimensions of 1270 mm × 1270 mm × 50 mm. As shown in Figure 9(c), maximum 9 out of 24 specimens would meet the criteria of density variation within 2% (see the 9%–11% band).

For the candidate material EV, 16 specimens were machined from three boards ("a" to "c") that produced in the same batch. Each board has nominal dimensions of 1200 mm × 600 mm × 50 mm. As shown in Figure 9(d), maximum 5 out of 16 specimens would meet the criteria of density variation within 2% (see the 2%–4% band).

The uniformity assessment of each candidate material, as seen in Figure 9, shows that the density variation is several fold worse than the 2% required in the measurement standard. Therefore, to meet the requirement for material uniformity, the specimens need to be selected to have a density variation within 2%. Figure 9 shows that for each material, some specimens have met the uniformity requirement.

3.   DISCUSSION

In order to assess the dimensional, mechanical, and chemical stabilities and uniformity of each candidate reference material, a test matrix has been performed on each of the selected materials. The tests in the matrix include material composition via XRF and XRD
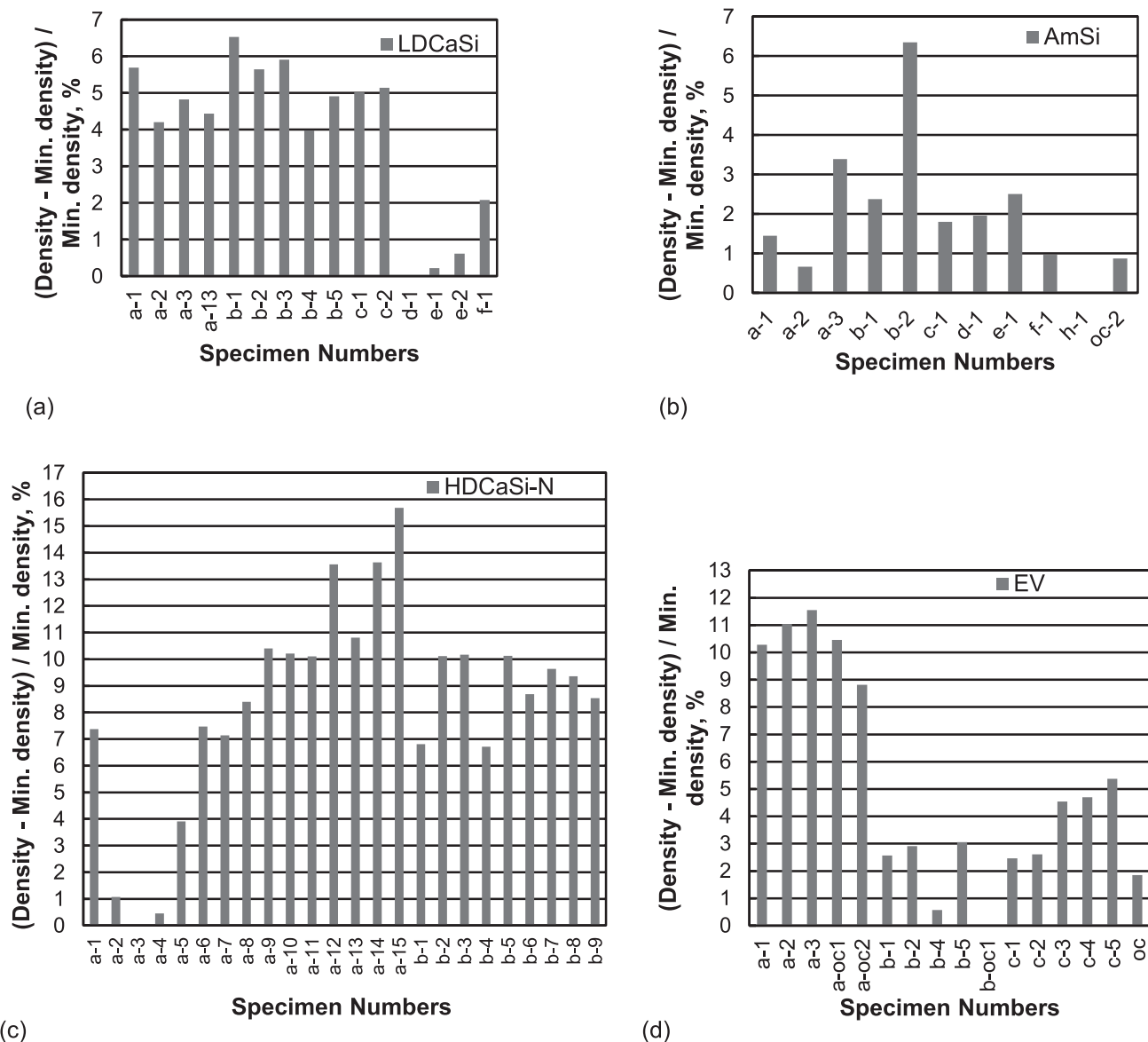
(a)

(b)

(c)

(d)

Figure 9. Material uniformity assessments via density variation.

analysis; microstructure via SEM; thermal expansion, thermal shrinkage of large specimens; TGA; DSC, analysis and density distribution.

The thermal expansion measurements on small specimens and thermal shrinkage measurements on large size specimens have provided a key indicator of the dimensional and mechanical stability of the materials. In thermal expansion measurements, all materials have shown permanent shrinkages on heating to 850°C and holding this temperature for 1 hour. All materials show irreversible changes in expansion behavior as a result of this exposure, which correspond with permanent changes to their respective microstructures. However, the microstructure of each material appears to remain stable after the first heat treatment.

The discussion below starts with the group of calcium silicate materials, then the EV and finally the amorphous silica insulation (AmSi).

Of the calcium silicate based materials, LDCaSi shows near isotropic behavior, but HDCaSi-N and HDCaSi-B are distinctly anisotropic, correlating with a strong texture in the as manufactured condition (see Figure 3 for the SEM of HDCaSi-N). From compositional data (Table 1), these products contain between 2% and 8% organic material before heating, and microstructurally there is evidence of the use of organic binders and inorganic fibers to help impart handling strength (see Figures 2 and 3). Clearly, organic components and combined water will burn out during heating and, as has been observed, inorganic fibers melt into the surrounding matrix (Figure 3). These changes on first

heating are clearly displayed by the behavior in TGA runs and by the signal characteristics seen in the DSC heat flow traces (see Figures 6–8). However, it is not the purpose of this study to interpret these changes in detail, but to focus on the longer term material stability under thermal cycling.

There are also significant differences in the inorganic compositions of these materials (see Table 1). LDCaSi and HDCaSi-N show lower SiO_2:CaO mass ratios than HDCaSi-B or the original NPL material, HDCaSi-HT3B. HDCaSi-B shows a tendency for dimensional instability at room temperature after heating, and this correlates with the likelihood of the undetected presence of a small amount of hydratable phase (possibly undetected CaO or a cement-like phase) in addition to stable anhydrous $CaSiO_3$ (wollastonite). This trend is absent in HDCaSi-N, which is closer to stoichiometric $CaSiO_3$ in overall composition. This trend is also absent in LDCaSi, which converts from xonotlite ($6CaO.6SiO_2.H_2O$) (US Patent, 1983; Zhang, Wei, & Yu, 2005) to wollastonite on heating.

The exfoliated vermiculite product EV is unstable on heating, and shrinks substantially with a high mass loss. After first heating the transition of the silica phase cristobalite is detectable in the thermal expansion behavior, although not within the complex XRD pattern of vermiculite, which is still the dominant species present. Commercial exfoliation processes use short dwell-time exposure to a temperature in excess of 540°C, but not as hot as the maximum used in the present experiments, providing a good explanation as to why the material might not be stable. In addition, any organic and inorganic binders will degrade during heating, adding to the instability of behavior.

The amorphous silica insulation AmSi is a very low density, weakly bonded material comprising silica and rutile, held together with a low volume fraction of aluminosilicate fibers. Heating to 850°C does not markedly change the structure, but removes a small amount of organic binder, resulting in an even weaker product and making it unsuitable as a robust reference material.

4.   CONCLUSION

Provisional assessments have been performed on a short list of four candidate high-temperature refractory type thermal conductivity reference materials: LDCaSi, AmSi, HDCaSi-N and EV, that were selected based on results of literature reviews and surveys that were carried out at the start of the "Thermo" project. Based on initial tests on the stability of material composition and microstructure, dimensional stability, mechanical stability, chemical stability, and uniformity, the two most promising candidate materials that would be suitable to be further developed into high-temperature thermal

conductivity reference materials in the next stage are LDCaSi and HDCaSi-N. Although permanent changes were observed during the first heat treatment, these two materials are dimensionally, mechanically, and chemically stable after the first heat treatment. In addition, the microstructures of these two materials appear to remain stable, and they are more robust and easier to handle. However, it is important that the specimens of reference materials meet the requirement for material uniformity, i.e., density varies within 2%; hence, there need to be a stringent selection process.

5.   FUTURE WORK

The next stage is to procure and select a batch of LDCaSi and HDCaSi-N specimens that meet the material uniformity requirement. Further detailed characterizations will be carried out on these specimens in terms of thermal conductivity and long term stability.

REFERENCES

CEN/TS 15548-1. (2014). *Thermal insulation products for building equipment and industrial installations. Determination of thermal resistance by means of the guarded hot plate method. Measurements at elevated temperatures from 100°C to 850°C.* London: The British Standard Institution.

Ebert, H., & Hemberger, F. (2011). Intercomparison of thermal conductivity measurements on a calcium silicate insulation material. *International Journal of Thermal Sciences, 50*, 1838–1844.

ISO Guide 34. (2009). *General requirements for the competence of reference material producers*. Geneva: International Organization for Standardization.

Salmon, D. R. (1996). The NPL high temperature guarded hot-plate. In K. E. Wilkes, R. B. Dinwiddie, & R. S. Graves (Eds.), *Proceedings of the 23rd International Thermal Conductivity Conference* (pp. 431–441). Lancaster, PA: Technomic Publishing Company, Inc.

Salmon, D. R. (2001). Thermal conductivity of insulations using guarded hot plates, including recent developments and sources of reference

materials. *Measurement Science & Technology, 12*, 89–98.

Salmon, D. R., Tye, R. P., & Lockmuller, N. (2009). A critical analysis of European standards for thermal measurements at high temperatures: I. History and technical background. *Measurement Science & Technology, 20*, 015101.

Tye, R. P., & Salmon, D. R. (2002). NPL initiatives in the development of thermal properties reference materials. *International Journal of Thermophysics, 23*(4), 1047–1061.

US Patent 4402892. (1983). *Method for making xonotlite insulation by foaming an aqueous slurry of calcareous and siliceous reactants and cellulosic and glass fibers.* Alexandria, VA: The United States Patent and Trademark Office (USPTO).

Wu, J., & Morrell, R. (2012). Corrections for thermal expansion in thermal conductivity measurement of insulations using the high-temperature guarded hot-plate method. *International Journal of Thermophysics, 33*, 330–341.

Wu, J., Salmon, D. R., Lockmuller, N., Stacey, C., & Gaal, D. S. (2010). Design, construction and performance checks of the NPL upgraded high temperature guarded hot plate. In P. S. Gaal (Ed.), *Proceedings of Thermal Conductivity 30/Thermal Expansion 18* (pp. 529–541). Lancaster, PA: DEStech Publications, Inc.

Zhang, X., Wei, G., & Yu, F. (2005). Thermal radiative properties of xonotlite insulation material. *Journal of Thermal Science, 14*(3), 281–284.

APPENDIX

The nominal dimensions of each specimen in mapping of density distribution are listed in Table A.1 below.

Table A.1. Nominal dimensions of each specimen.

Nominal dimensions (mm)	LDCaSi	AmSi	HDCaSi-N	EV
$500 \times 500 \times 50$	a-1, b-1, d-1, e-1, e-2, f-1	c-1, d-1, h-1	a-1, a-6, a-7, a-9, a-10, a-15, b-1, b-9	a-1, b-1
$300 \times 300 \times 50$	a-2, a-3, b-2, b-3	a-1, b-1, c-1	a-2, a-3, a-4, a-5, a-8, a-13, b-2, b-3, b-4, b-5, b-7, b-8	a-2, a-3, a-oc1, a-oc2, b-2, b-oc1, c-1, c-2, c-3, c-4
$\varnothing 310 \times 50$	c-1, c-2	f-1	b-6	c-5
$300 \times 200 \times 50$	b-3, b-4	a-2, a-3	a-11, a-14	b-4, b-5
$200 \times 200 \times 50$	-	oc-2	–	–
$100 \times 100 \times 50$	a-13	b-2	a-12	oc